Soft Matter

COMMUNICATION

View Article Online
View Journal

Electrically-tunable surface deformation of a soft elastomer†

Samuel Shian* and David R. Clarke

Cite this: DOI: 10.1039/c6sm00090h

Received 13th January 2016,
Accepted 1st March 2016

DOI: 10.1039/c6sm00090h

www.rsc.org/softmatter

Published on 01 March 2016. Downloaded by Harvard University on 09/03/2016 23:04:24.

The flat surface of a thin elastomer on a conducting substrate can be deformed by applying an electric field to a percolating network of metallic nanowires randomly dispersed over the surface. The magnitude of the field-induced surface undulations increases with the applied field and can locally be several times the diameter of the nanowires. Optical imaging indicates that the effect is reversible and the surface flatness is recovered when the electric field is removed. It is found that it is the field-induced changes in the surface morphology rather than the nanowires themselves that strongly scatter light. The optical effects could be exploited in functional devices including tunable privacy windows, displays, and camouflage. There is also the potential for tuning the adhesion of elastomers to other materials.

The surface morphology of elastomers and polymers can be altered in a number of ways, for instance by exposure to different chemical environments, applying an external force, by changing the temperature, or, for some materials, by applying an electric field. These are typically slow processes and the surface deformations produced are often irreversible. For instance, when PDMS is exposed to ionizing radiation, such as a gas plasma used to increase adhesion to its surface, it wrinkles in response to the shrinkage in the near-surface region.[1,2] Similarly, swelling of a laterally confined polymer film exposed to a solvent, whether on a solid or liquid substrates, can create wrinkle patterns.[3] Wrinkling also can be produced by exploiting large strain incompatibility between different materials, such as metallic films on an elastomeric surface, in response to changes in temperature.[4,5] Recent studies have used an electric field to induce electromechanical instabilities, leading to deformation on the surface.[6–10] In some cases, the deformation is quite fast;[7,11] however, the use of a highly conducting, thick liquid electrolyte as an electrode limits its practicality. In this work, we describe an alternative, more rapid as well as reversible process based on electric field controlled electrostatic interactions across the thickness of a thin sheet of an elastomer. The magnitude of the resulting surface deformations can be controlled by the variation of the applied electric field. As an example for the utility of being able to control the surface morphology of an elastomer, we demonstrate that the reflectance and transmission of light incident on a tunable surface can be modulated.

During the course of our work utilizing percolative networks of SWCNT and silver nanowires as compliant, electrically conducting electrodes for dielectric elastomer actuators[12] and energy harvesting systems,[13,14] we noticed that the surface deformed slightly when an electric field was applied to the electrodes. To investigate this observation systematically, we fabricated a simple layered structure consisting of a thin sheet of elastomers attached to an ITO coated soda-lime glass substrate with a thin layer of randomly oriented silver nanowires on top. The elastomer, a polyacrylate (3M VHB 4905) sheet of nominal thickness 500 μm, was first pre-stretched biaxially to 300% linear strain, producing a sheet of 31 μm thickness. The thinned elastomer sheet was then attached onto an ITO-coated glass with care being taken to avoid trapping of any air. Silver nanowire (AgNW) electrodes with a target areal density of 78 mg m^{-2} were prepared from an ethanol suspension (90 nm average diameter, 20–60 μm length, SLW-NW-90, Blue Nano, Charlotte, NC), cast through a Teflon filter and then transferred to the surface of a thin elastomer sheet.[12] The nanowire network was connected to a high-voltage source with the other electrode being the conducting substrate. With the increasing voltage, the surface deformed, as shown in the optical micrographs of Fig. 1 and in the confocal images of Fig. 2.

When connected to a voltage source, the nanowire network charges and is attracted by electrostatic forces to the oppositely charged ITO electrode. For a uniformly distributed charge on the surface of a dielectric having a permittivity, ε, the force acting on the surface is the Maxwell stress tensor $\boldsymbol{\sigma}$. In the absence of a magnetic field, this can be expressed as:[15,16]

$$\boldsymbol{\sigma} = \varepsilon \boldsymbol{E}\boldsymbol{E} - 1/2\varepsilon(\boldsymbol{E}\cdot\boldsymbol{E})\boldsymbol{I} \quad (1)$$

John A. Paulson School of Engineering and Applied Sciences, Harvard University, 29 Oxford Street, Cambridge, MA 02138, USA. E-mail: sshian@seas.harvard.edu

† Electronic supplementary information (ESI) available. See DOI: 10.1039/c6sm00090h

Published on 01 March 2016. Downloaded by Harvard University on 09/03/2016 23:04:24.

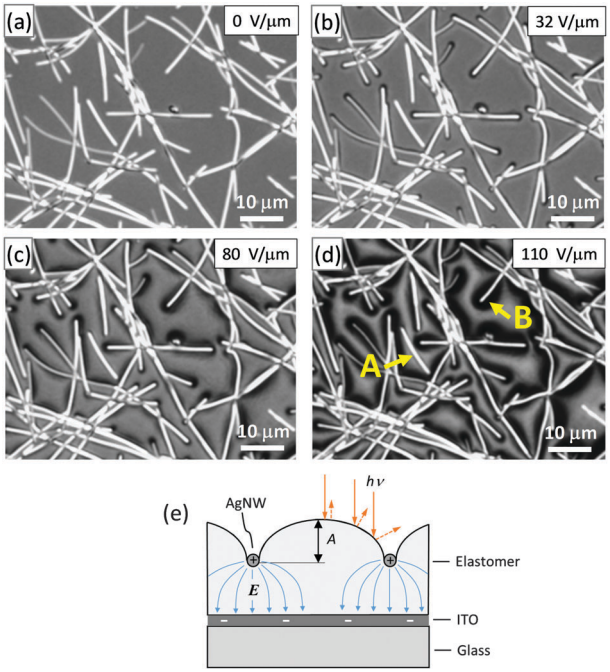

Fig. 1 (a) Bright field optical microscopy image showing the spatial distribution of the silver nanowires and the surface of the elastomer in between. The areal density of nanowires is ~78 mg m^{-2}. (b)–(d) The same region at the indicated electric fields (nominal) showing the field-induced local deformations of the elastomer surface revealed by optical contrast change. (e) A schematic cross-section of the surface displacements and the electric field emanating from individual nanowires.

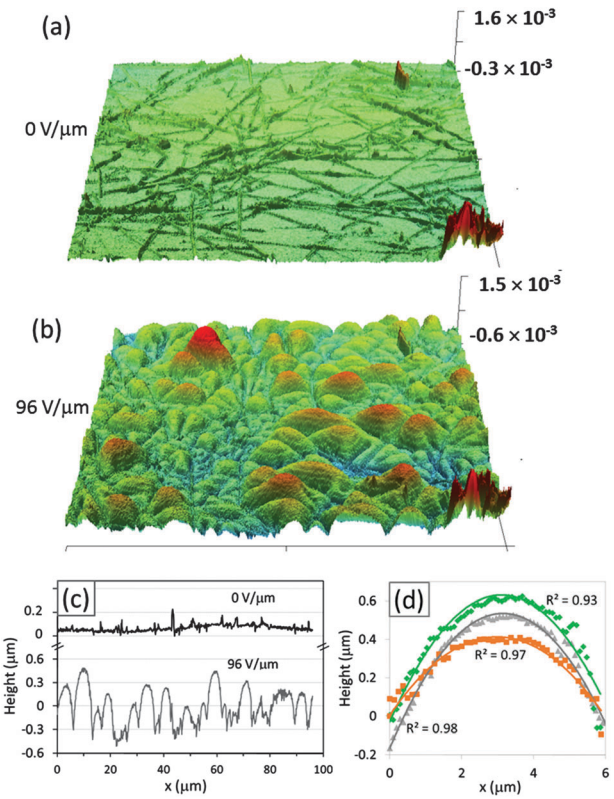

Fig. 2 Confocal microscopy maps of the nanowire electrode and the elastomer surface. (a) Without any field and (b) at an applied electric field (nominal) of 96 V μm^{-1}. The scanned area is 96 × 96 μm^2. (c) Line profiles show that the surface morphology is much rougher and in places can be several times the diameter of the silver nanowires (diameter 90 nm) when the voltage is applied. The dips in the lower trace correspond to the locations of individual nanowires. (d) Detailed fitting of the surface bulges formed between two nearly parallel nanowires. These profiles can be fit reasonably well using parabolic equation (solid lines).

where $\boldsymbol{E}$ is the electric field and $\boldsymbol{I}$ is the identity tensor. The direction of the Maxwell stress at any point on the surface is parallel to the direction of the local electric field, which is, in turn, perpendicular to the interface of the conductor and dielectric. This electric field is depicted by the lines emanating from the nanowires to the other electrode interface, as shown schematically in Fig. 1e. At the interface of dielectric and nanowires, the normal force is $F_n = \boldsymbol{n}\cdot\boldsymbol{\sigma}\cdot\boldsymbol{n} = 1/2\varepsilon\boldsymbol{E}\cdot\boldsymbol{E}$, and the tangential force is $F_t = \boldsymbol{t}\cdot\boldsymbol{\sigma}\cdot\boldsymbol{n} = 0$, where n and t are the unit normal and tangential vectors to the interface of nanowires/elastomer, respectively. Because of the random distribution of nanowires in the plane of the surface, the electric field is not uniform over the surface but is the highest immediately under the individual nanowires. Furthermore, as the cross-section of the silver nanowires are distorted pentagons,[17] there is a further enhancement of the electric field around the edge of the nanowires. Nevertheless, the simpler case of the force between a charged cylindrical wire parallel to an infinite conducting plane and embedded in a uniform dielectric expresses the principal dependencies. For this case, the attractive force per unit length of wire, F_n/l, acting towards the conducting plane, can be written as:[18]

$$F_n/l = \frac{\pi\varepsilon}{4a^2}\frac{\Phi^2}{[\cosh^{-1}(H/R)]^2} \quad (2)$$

where Φ is the potential, H is the distance between the axis of wire and the plane, and R is the wire radius, and $a = 1/2\left(H + \sqrt{H^2 - R^2}\right)$. This attractive force deforms the elastomer locally altering its surface morphology. In the following experiments, the electric field is reported as nominal values, defined as the applied voltage divided by the initial thickness of the elastomer, rather than the instantaneous thickness.

Unlike the nanowires, the ITO conducting surface is a continuous coating on a much thicker, solid, glass substrate. Consequently, the substrate imposes a mechanical constraint on the lateral expansion of the elastomer which, being an incompressible material, cannot change in volume. So, when the nanowires are charged by applying a voltage their displacement towards the ITO coated glass substrate produces an average displacement of the elastomer between the nanowires in the opposite direction in order to conserve the overall volume of the elastomer. The displacement of the elastomer surface varies spatially because of the inhomogeneous distribution of the randomly distributed nanowires as can be seen in the bright field reflection optical microscopy by comparing the images in Fig. 1 before and during the application of an electric field. Dark outlines along the length of the nanowires indicate that light is reflected at an angle away from the incident illumination by the local curvature of the deformed elastomer surface. These dark

 This journal is © The Royal Society of Chemistry 2016

Published on 01 March 2016. Downloaded by Harvard University on 09/03/2016 23:04:24.

outlines diminish away from the nanowires indicating that the surface has bulged upwards in between. Comparison of the individual images also shows that the lateral positions of the individual nanowires are unchanged as the electric field is applied. Another feature of the images is that as the applied electric field is increased, the optical contrast becomes more pronounced especially at the ends of the nanowires, as illustrated by the 'B' arrow in Fig. 1d. Also, unless the nanowires are close together, the optical contrast is symmetrical about the axis of the nanowires. A notable feature of the images is that the elastomer surface is not deformed in the immediate vicinity of the individual nanowires that are not connected to the percolating network. These can be identified by the nanowires that are not outlined by a band of dark contrast, for instance, the one marked by the 'A' arrow in Fig. 1d.

Confocal microscopy (Model VK-X200, Keyence Corp. with a 405 nm laser) was used to quantify the surface deformations as a function of the applied electric field. The results are illustrated in Fig. 2. Before an electric field is applied, the elastomer surface is relatively flat and the main contributions to the roughness are from the individual silver nanowires on the surface. Quantitative surface profiles indicate that the peaks have heights in the range of 80 to 170 nm, which correspond to a single and two overlapping nanowires, respectively (Fig. 2c). With the application of an electric field, the morphology of the elastomer surface changes continuously, producing deep depressions at the individual nanowires and bulges in between the individual nanowires. The maximum peak-to-valley displacements were more than 600 nm for an applied nominal field of 96 V μm^{-1} indicating that the nanowires are displaced towards the ITO electrode by many times their diameter (Fig. 2d). The magnitude of the surface displacement also varies with the position, depending on the spacing between adjacent percolating nanowires; relatively small vertical displacements occurred where the spacing between the nanowires was small whereas where their spacing was larger, the relative heights of the bulges were larger. Sampling of the surface profiles of the elastomer between two adjacent and nearly parallel nanowires indicates that they are, to a good fit, parabolic. This is illustrated by the profiles shown in Fig. 2d.

Although the optical images, such as those shown in Fig. 1, reveal local variations in the surface as an electric field is applied as well as the association with individual nanowires, providing some physical insight, the random arrangement of the nanowires makes it difficult to establish the overall deformation of the surface. An alternative, more effective measurement of the overall response can be monitored from variations in the transmitted light with the applied electric field. An example is shown in Fig. 3a using the optical arrangement in Fig. S1(a) (ESI†). In this measurement, the combination of collimating lenses and the 50 mm spacing between the sample and the detector allows for the detection of the in-line transmittance and the rejection of most of the scattered rays. The data, Fig. 3a, indicate that the majority of the incident illumination is transmitted diffusely as the electric field is increased. The broad dip in transmission in the 400–500 nm spectral range (Fig. 3a) is

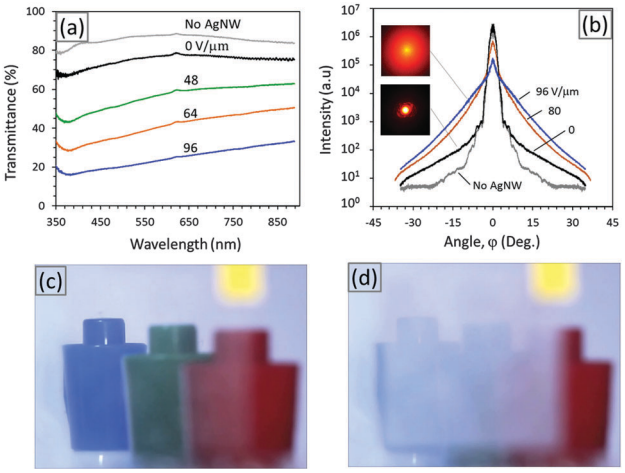

Fig. 3 (a) In-line spectral transmittance for different applied nominal fields. There is a slight absorption centered at about 360 nm, which is attributed to the plasmon resonance in the silver nanowires. (b) Angular distribution of the transmitted laser light (632 nm). The broadening is increased substantially as the surface deforms when the electric field is increased. This is also seen qualitatively in the recorded images in the inset. (c) A demonstration of light scattering is shown by the change in the clarity of the objects placed behind the sheet (c) before and (d) after the application of the field of 130 V μm^{-1}. Upon removal of the field, the sheet immediately returns to its initial, transparent condition. The electrode area is square, as shown by the white opaque area in (d) and is connected to an external power supply through the yellow tab in the upper right. The measurement setups for (a and b) and the real-time video of (c and d) are shown in Fig. S3 and Video S1 in the ESI,† respectively.

attributed to the excitation of the localized surface plasmon resonance in the silver nanowires.[19]

The angular dependence of the transmitted intensity was measured using a 2D detector in the arrangement shown in Fig. S1(b) (ESI†). A highly collimated He–Ne laser (1 mm diameter) was shone through the sample and detected using a 2D CMOS sensor (15.6 × 23.5 mm, model NEX-3N, Sony Corp.) placed on a translation stage, at a distance of 22 mm from the sample, to enable measurements up to large angles. Images were captured in a RAW mode at different exposure times to allow for the large dynamic range of the intensities. The pixel intensities were extracted using ImageJ software[20] and plotted as a function of the radial distance from the center of the beam. After collating the data together from multiple exposures and positions, the resulting angular dependence was determined. An example is shown in Fig. 3b, which compares the angular scattering from the surface roughness of the elastomer, the additional scattering from the silver nanowires and the scattering when electric fields of 80 and 96 V μm^{-1} are applied. The data plotted in Fig. 3b clearly show a broadening of the angular distribution in transmitted intensity as the electric field is increased. In the absence of the silver nanowires, the angular distribution is the intrinsic angular width of the laser beam and most of its intensity is confined within $\pm 5^{\circ}$. There are some weak diffraction peaks around the shoulder of the center beam, which originate from multiple interferences between the neutral density filters and the elastomer layers. When an electric field is applied, the

Published on 01 March 2016. Downloaded by Harvard University on 09/03/2016 23:04:24.

angular profiles become much broader, and the intensity at high angles increases at the expense of the intensity at the center beam. At a nominal electric field of 96 V μm^{-1}, the center (peak) intensity decreases by an order of magnitude, while the intensity at high angles increases by more than an order of magnitude out to $\sim$15 degrees. The integrated intensity of the peak ($<5^\circ$) represents the in-line transmission in Fig. 3a. Visually, the broadening of the transmitted beam is evident from the photographs of the transmitted laser beam shown in the inset in Fig. 3b. A demonstration of a tunable light diffuser is shown by placing objects behind an elastomer sheet, as shown in Fig. 3c and d. These marker cap objects are placed at 110, 220, and 330 cm from the sheet, where the left one is the furthest. In the absence of an electric field, the elastomer sheet is highly transparent and the objects can be clearly seen through it. After the application of an electric field of 130 V μm^{-1}, the sheet became hazy and the objects could no longer be clearly seen. The transparency of the sheet returns to its initial state upon removal of the field. The transition occurs relatively fast, at around 200 ms, and is reproducible, as shown by the real-time Video S1 in the ESI.† The switching speed of the transition may be affected by several factors, which include charge re-distribution (or RC) time constant and viscoelasticity of the elastomer.[21] It is suspected however that the viscoelasticity of an acrylic elastomer could be the major limiting factor and therefore the switching speed may be improved using a low viscoelastic elastomer, such as silicone.

The angular spread in transmitted intensity and its variation with an electric field are due to the combination of different mechanisms. One is the optical scattering from the individual nanowires, a form of Rayleigh–Gans scattering,[22] that scales with their shape and diameter. A second contribution is the optical interference between nanowires, in particular in those regions where the nanowires are close together, a configurational dependent scattering. A third possible contribution is the refraction of the incident illumination by the local variations in the surface morphology. As the optical and confocal images indicate that the lateral positions of the nanowires do not change with the applied electric field, it can be concluded that the first two contributions cannot significantly affect the increase in angular scattering with the electric field. Consequently, the refraction term, which does depend on the electric field induced force on the nanowires, is the major contribution to the angular broadening of the transmitted beam. Although the shape of the elastomer surface in the immediate vicinity of the nanowires is unknown because of the finite resolution of the confocal images, the shape at a distance a few wavelengths away can be approximated, as shown from the confocal images, by a parabolic surface. Simple ray tracing based on the refraction and reflection from parabolic surfaces, assuming no diffraction, leads to angular broadening that increases as the amplitude of the parabolic bulge increases. This is consistent with the observed angular broadening. In this simple model, however, the maximum spread angle of the rays is determined by the maximum curvature of the parabola. Between these limits, the shape of the angular profile is an inverted projection

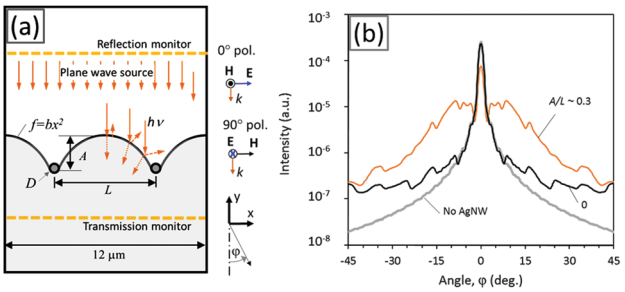

Fig. 4 (a) Schematic of the FDTD 2D-simulation setup used to calculate the angular distribution profile from a regularly spaced, L, parallel nanowires with diameter D, and surface undulations with amplitude A. (b) The results of simulation show the transmission as a function of the spread angle, φ. The transmission is averaged from 4 different spacings (1 μm, 2 μm, 6 μm, and 12 μm) and each at similar relative bulge amplitudes ($A/L \sim 0.3$).

of the parabolic bulge. Beyond this maximum angle, rather than decaying monotonically as observed in Fig. 3b, the intensity of refracted rays decreases sharply to zero, except when the amplitude of bulges is high enough that multiple refraction occurs, spreading the rays to the higher angle.

Quantitative modeling, taking into account diffraction effects and features sizes, was performed based on solving Maxwell's equations using the finite difference time-domain software (FDTD Solutions v8.12, Lumerical Solution Inc., Canada). The simulation cell is shown in Fig. 4a and consists of parallel nanowires, diameter R, with a lateral spacing, L, with the surface deformation in between given by a parabolic function ($f = bx^2$) with an amplitude, A, that depends on the magnitude of the applied electric field. (In principal, as the force on an individual nanowire is known from eqn (2), the resulting surface shape can be computed. However, this is difficult because of electromechanical coupling between the local electrostatic attraction and the mechanical response of the elastomer. This is further complicated by the fact that the elastomer is a hyper-elastic solid so the coupling is intrinsically non-linear.)

The left and the right sides of the simulation box are periodic boundaries while the top and bottom sides are perfectly absorbing boundaries. The width of the simulation box is fixed at 12 μm, which may contain one or multiple periodic structures, depending on the nanowire spacing L. The optical properties of the elastomer were assumed to be the same as those of silica (SiO_2). The optical data of silver and SiO_2 were taken from Palik.[23] Power-frequency monitors, positioned 500 nm below, and 2.5 μm above, the center of the nanowires, are used in the simulation to determine the transmission and reflection at each wavelength. The angular intensity of the light is calculated using far-field projection from Poynting vectors that pass through the monitors.[24] To smooth out the diffraction effects due to the periodicity in the simulation cell, the angular intensity profile was averaged over 150 profiles from different wavelengths in the visible range (400–900 nm). This averaging removes all the diffraction minima, except for the first minima that separate the zeroth and first diffraction orders. The simulation for each geometrical setup was performed twice, using 0° and 90° polarization light sources and the results are averaged to

 This journal is © The Royal Society of Chemistry 2016

Published on 01 March 2016. Downloaded by Harvard University on 09/03/2016 23:04:24.

represent a non-polarized light source. The simulated angular scattering profiles for two different spacing (L = 2 μm and 6 μm) of nanowires are shown in Fig. S3 (in the ESI†). Finally, the angular intensity is averaged from four different spacing of nanowires (L = 1 μm, 2 μm, 6 μm, and 12 μm) with each at similar relative bulge amplitudes ($A/L \sim 0.3$), as shown in Fig. 4b. In the final averaging, it was assumed that the area fraction of the nanowires was unchanged. In these averaged simulation profiles, the in-line transmittance is represented by the central region, which is peaked at 0°. All the intensity at higher angles is due to scattering and refraction.

Although approximate, the comparison in Fig. 4b exhibits many of the essential features of the observed optical scattering in Fig. 3b. This is despite neglecting several effects, such as those due to the initial shape of the laser beam, spatial variations in the surface deformation, intrinsic roughness of the surface before actuation, the deformation around the ends of the nanowires, as well as the existence of the second air–elastomer interface at the exit surface. The simulations show that as the amplitude of the surface deformation increases, the intensity of diffused transmittance increases, accompanied by a decrease in the in-line transmittance. A similar trend is also observed in the reflected beam (shown in Fig. S3 in the ESI†) although the overall reflected intensity is more than an order of magnitude less. The simulations show general agreement with the experiment in that the silver nanowires cause scattering at large angles, above 10° (compare Fig. 3b and 4b). Such scattering is more intense on the reflection side, as expected for metallic structures. In both cases, the intensity of the scattered beam increases as the concentration of nanowires increases. Comparison of the simulations in the absence of nanowires or using nanowires having the optical properties of the glass instead of silver indicates that the metallic contribution of the silver nanowires to the scattering is relatively constant, regardless of the magnitude of the surface deformation (Fig. S2 in the ESI†). At large deformations, the majority of the scattering in transmission is caused by the bulge geometry, rather than by the silver nanowires.

Summary

We have shown that when a percolating network of nanowires on a soft elastomer is electrically charged it is attracted to an underlying conductor causing a spatially non-uniform surface deformation of the elastomer dielectric. The local surface displacements increase with the electric field and can be many times the diameter of the nanowires. The field-induced surface undulations also strongly scatter visible light leading to an angular broadening of the transmitted light that increases with the applied electric field. These deformation effects are fully reversible. Practical applications of the field-induced surface deformation include tunable privacy windows, smart glass, projector screens, displays, and camouflage. Outside of optics, the ability to electrically tune the surface deformation may be potentially useful in areas such haptics, adhesion controls, and functional surfaces.

Acknowledgements

This work was supported by the National Science Foundation through the grant CMMI-1333835 and in part by the MRSEC program of the National Science Foundation under award number DMR 14-20570. The authors would like to thank William Peabody of Keyence Corp. for assistance with the confocal microscopy and Peter Kjeer for facilitating the measurements.

References

1 J. Y. Chung, J. P. Youngblood and C. M. Stafford, *Soft Matter*, 2007, **3**, 1163.
2 D. B. H. Chua, H. T. Ng and S. F. Y. Li, *Appl. Phys. Lett.*, 2000, **76**, 721.
3 E. P. Chan, E. J. Smith, R. C. Hayward and A. J. Crosby, *Adv. Mater.*, 2008, **20**, 711–716.
4 N. Bowden, S. Brittain and A. Evans, *Nature*, 1998, **393**, 146–149.
5 J. Kim and H. H. Lee, *J. Polym. Sci., Part B: Polym. Phys.*, 2001, **39**, 1122–1128.
6 D. Van Den Ende, J. D. Kamminga, A. Boersma, T. Andritsch and P. G. Steeneken, *Adv. Mater.*, 2013, **25**, 3438–3442.
7 Q. Wang, L. Zhang and X. Zhao, *Phys. Rev. Lett.*, 2011, **106**, 118301.
8 N. Arun, A. Sharma, P. S. G. Pattader, I. Banerjee, H. M. Dixit and K. S. Narayan, *Phys. Rev. Lett.*, 2009, **102**, 1–4.
9 N. Wu and W. B. Russel, *Nano Today*, 2009, **4**, 180–192.
10 E. Schaffer, T. Thurn-Albrecht, T. P. Russell and U. Steiner, *Nature*, 2000, **403**, 874–877.
11 B. Xu and R. C. Hayward, *Adv. Mater.*, 2013, **25**, 5555–5559.
12 S. Shian, R. M. Diebold, A. McNamara and D. R. Clarke, *Appl. Phys. Lett.*, 2012, **101**, 061101.
13 J. Huang, S. Shian, Z. Suo and D. R. Clarke, *Adv. Funct. Mater.*, 2013, **23**, 5056–5061.
14 S. Shian, J. Huang, S. Zhu and D. R. Clarke, *Adv. Mater.*, 2014, **26**, 6617–6621.
15 A. Dorfmann and R. W. Ogden, *J. Elastoplast.*, 2006, **82**, 99–127.
16 Q. Wang, Z. Suo and X. Zhao, *Nat. Commun.*, 2012, **3**, 1157.
17 Y. Sun, Y. Ren, Y. Liu, J. Wen, J. S. Okasinski and D. J. Miller, *Nat. Commun.*, 2012, **3**, 971.
18 R. Fitzpatrick, *Maxwell's Equations and the Principles of Electromagnetism*, Jones & Bartlett Learning, 2008.
19 P. Spinelli and A. Polman, *ACS Nano*, 2012, **12**, 3138–3144.
20 W. S. Rasband, *ImageJ*, U.S. National Institutes of Health, Bethesda, Maryland, USA, 2015, http://imagej.nih.gov/ij/.
21 L. Maffli, S. Rosset, M. Ghilardi, F. Carpi and H. Shea, *Adv. Funct. Mater.*, 2015, **25**, 1656–1665.
22 H. C. van de Hulst, *Light Scattering by Small Particles*, Dover, 1957.
23 *Handbook of Optical Constants of Solids*, ed. E. D. Palik, Academic Press, Burlington, 1997.
24 FDTD Solution Knowledge Base (User manual), Lumerical Solutions, Inc, 2015.